inorganics

MDPI

Article

Organoruthenium Complexes Containing Phosphinodicarboxamide Ligands

Roberto Nolla-Saltiel [1,2,*], Ana M. Geer [1,3,*], Helen R. Sharpe [1], Cameron D. Huke [1], Laurence J. Taylor [1], Thomas G. Linford-Wood [1], Ashleigh James [1], Jamie Allen [1], William Lewis [1,4,5], Alexander J. Blake [1], Jonathan McMaster [1] and Deborah L. Kays [1,*]

1 School of Chemistry, University of Nottingham, University Park, Nottingham NG7 2RD, UK
2 Department of Chemistry, Queen's University, Kingston, ON K7L 3N6, Canada
3 Instituto de Síntesis Química y Catálisis Homogénea (ISQCH), Departamento de Química Inorgánica CSIC, Universidad de Zaragoza, Pedro Cerbuna 12, 50009 Zaragoza, Spain
4 School of Chemistry, The University of Sydney, F11, Eastern Avenue, Sydney, NSW 2006, Australia
5 Sydney Analytical, The University of Sydney, F09, Eastern Avenue, Sydney, NSW 2006, Australia
* Correspondence: roberto.nollasaltiel@queensu.ca (R.N.-S.); anageer@unizar.es (A.M.G.); deborah.kays@nottingham.ac.uk (D.L.K.)

Abstract: Ruthenium complexes of phosphinocarboxamide ligands, and their use to form metallacycles using halide abstraction/deprotonation reactions are reported. Thus, [Ru(*p*-cym){$PPh_2C(=O)NHR$}Cl_2; R = ^{i}Pr (**1**), Ph (**2**), *p*-tol (**3**)] and [Ru(*p*-cym){$PPh_2C(=O)N(R)C(=O)N(H)R$}Cl_2; R = Ph (**4**), *p*-tol (**5**)] were synthesized from [(*p*-cym)$RuCl_2$]$_2$ (*p*-cym = *para*-cymene) and phosphinocarboxamides or phosphinodicarboxamides, respectively. Single-crystal X-ray diffraction measurements on **1**–**5** reveal coordination to ruthenium through the phosphorus donor, with an intramolecular hydrogen bond between the amine-bound proton and a metal-bound chloride. Six-membered metallacycles formed by halide abstraction/deprotonation of complexes **4** and **5** afforded [Ru(*p*-cym){κ^2-*P,N*-$PPh_2C(=O)N(R)C(=O)NR$}Cl] [R = Ph (**6**), *p*-tol (**7**)]. These species exist as a mixture of two rotational isomers in solution, as demonstrated by NMR spectroscopy.

Keywords: phosphinocarboxamide; metallacycle; ruthenium; P ligands; coordination chemistry

Citation: Nolla-Saltiel, R.; Geer, A.M.; Sharpe, H.R.; Huke, C.D.; Taylor, L.J.; Linford-Wood, T.G.; James, A.; Allen, J.; Lewis, W.; Blake, A.J.; et al. Organoruthenium Complexes Containing Phosphinodicarboxamide Ligands. *Inorganics* **2023**, *11*, 372. https://doi.org/10.3390/inorganics11090372

Academic Editors: Koichiro Takao, Wolfgang Linert, Gabriel García Sánchez and David Turner

Received: 24 August 2023
Revised: 7 September 2023
Accepted: 12 September 2023
Published: 19 September 2023

1. Introduction

Ligands incorporating both hard and soft donor atoms continue to attract attention [1] and have found applications in coordination chemistry [1–3], biomedicine [4,5], enantioselective catalysis [6,7] and supramolecular and self-assembled arrays [8]. Recently, we reported the syntheses of functionalized phosphinocarboxamides (PCAs) and a new family of phosphinodicarboxamides (PDCAs) through the catalytic hydrophosphination of isocyanates (**L-1**–**L-5**) [9]. These compounds possess hard (N or O) and soft (P) donor atoms that enable their binding to a wide range of metal centres in diverse coordination modes [10]. Despite this, PCAs have found limited use as ligands [1–3,11] and PDCAs have not been investigated in metal complexation reactions. Relevant co-ordination chemistry includes (i) the di-insertion of phenyl isocyanates into an amine bond using lanthanide metal centres to form $Cp_2Ln\eta^2$:η^1-PyNCON(Ph)CONHPh] (Ln = Yb, Er, Y, Dy, Gd; Py = 2-pyridyl), from which substituted ureas can be prepared [12]; (ii) the use of primary phosphinocarboxamides in the syntheses of *cis*-$[Mo(CO)_4(PH_2C(=O)NH_2)_2]$ [11] and [Ru(*p*-cym){$PH_2C(=O)N(H)Cy$}Cl_2] (Cy = cyclohexyl) [2]; and (iii) the reaction of Fe(η^5-$C_5H_4N(H)C(=O)PPh_2)_2$ with $PtX_2(PPh_3)_2$ (X = Cl, Br) that has allowed for the first selective synthesis of M_4L_6 cage complexes, facilitated by hydrogen bonding interactions between the PCA moiety and the halide ion [13].

Half-sandwich ruthenium complexes have been widely studied as potential catalysts [14–23], due to their ease of interconversion to other Ru(0) and Ru(II) complexes [17].

In particular, [(η^6-arene)$RuCl_2(PR_3)$] (R = aryl or alkyl) [10] complexes are effective precursors for a variety of catalytic and stoichiometric organic transformations [18,24]. Notable examples include the transfer hydrogenation of ketones and benzaldehydes by [Ru(*p*-cym){OC_6H_4-2-$CH_2NHC_6H_4$-*p*-Me}Cl] [15,16,25], the isomerization of olefins such as allylbenzene and 1-octene by [Ru(*p*-cym)*L*Cl] {*L* = 4-(phenylazo)resorcinol} [14], and a wide range of heteroatom insertion reactions involving cationic allenylidene and cumulenylidene complexes such as [Ru=(C=C=CPh_2)(η^5-1,2,3-$Me_3C_9H_4$)(CO)PPh_3)]$^+$ [21]. Thus, the *p*-cymene-ruthenium(II) fragment is an ideal choice for probing the coordination chemistry of new PDCAs, and for comparisons with the analogous PCA-containing complexes.

Herein, we describe the syntheses of [Ru(*p*-cym){$PPh_2C(=O)NHR$}Cl_2; R = ^{i}Pr (**1**), Ph (**2**), *p*-tol (**3**)] and [Ru(*p*-cym){$PPh_2C(=O)N(R)C(=O)N(H)R$}Cl_2; R = Ph (**4**), *p*-tol (**5**)]. This study includes the first reported examples of PDCAs as monodentate and bidentate ligands, with the latter coordination mode resulting in six-membered metallacycles.

2. Results and Discussion

*2.1. Synthesis and Characterization of [Ru(p-cym){$PPh_2C(=O)N(H)R$}Cl_2] [R = ^{i}Pr (**1**), Ph (**2**), p-tol (**3**)] and [Ru(p-cym){$PPh_2C(=O)N(R)C(=O)N(H)R$}Cl_2] ([R = Ph (**4**), p-tol (**5**)]*

A solution of [Ru(*p*-cym)Cl_2]$_2$ and **L-1** ($PPh_2C(=O)N(H)^iPr$) in a 1:2 ratio in dichloromethane was stirred at room temperature overnight, which, after removal of solvent and extraction into toluene afforded **1** as a dark red solid (Scheme 1). The use of phosphinocarboxamides with nitrogen-substituted aromatic groups (**L-2** and **L-3**) affords the analogous compounds [Ru(*p*-cym){$Ph_2PC(=O)N(H)R$}Cl_2; R = Ph (**2**) and *p*-tol (**3**)] (Scheme 1). Pure samples of **1**–**3** were isolated in moderate to excellent yields (**1**, 39%; **2**, 53%; **3**, 99%). These compounds exist as bright-red crystalline solids and have been characterized by NMR and IR spectroscopies, mass spectrometry, single-crystal X-ray diffraction and elemental analyses (see Supporting Information for full details and the Further Observations section for additional insights).

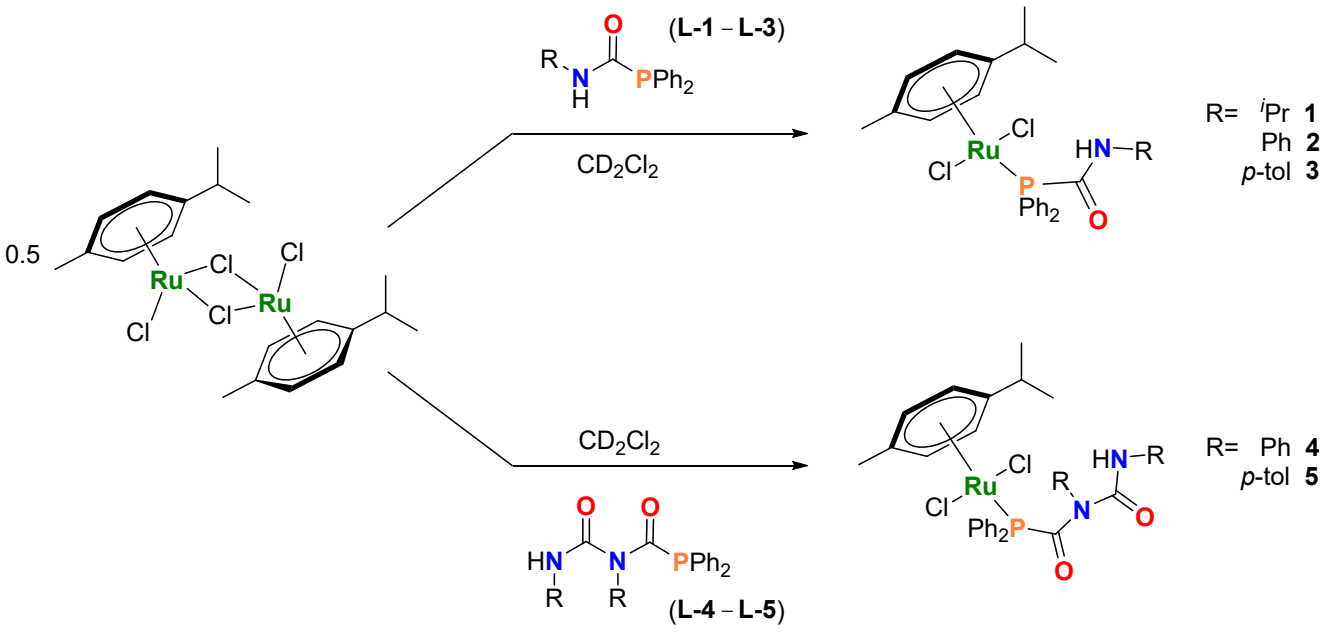

Scheme 1. Synthesis and structure of **1**–**5**. Reaction conditions: 0.5 eq. [Ru(*p*-cym)Cl_2]$_2$ and 1 eq. **L-1**–**L-5** at room temperature, 10 min.

In parallel, the phosphinodicarboxamides $PPh_2C(=O)NPhC(=O)NHR$ (R = Ph **L-4**, *p*-tol **L-5**) [9] were reacted with [Ru(*p*-cym)Cl_2]$_2$ (Scheme 1) under similar conditions, affording [Ru(*p*-cym){$PPh_2C(=O)N(R)C(=O)N(H)R$}Cl_2]; {R = Ph (**4**) and *p*-tol (**5**)}. Unlike **1**–**3**, complexes **4** and **5** are sparingly soluble in low-polarity hydrocarbons such as benzene

and toluene. Characterization using NMR spectroscopy in CD_2Cl_2 indicate only one species in solution for compounds **1**–**5** (Tables 1 and S1 and Figures S6–S15). These compounds possess bilateral symmetry in the *p*-cymene ligand as shown by ^{1}H and $^{13}C\{^{1}H\}$ NMR spectroscopic determinations in solution. Thus, in the $^{13}C\{^{1}H\}$ NMR spectra of **1**–**5**, the non-quaternary carbons of the *p*-cymene appear as two doublets, due to scalar coupling with the phosphorus atom of the PCA/PDCA ligand ($^{2}J_{CP}$ = 4 and 6 Hz; see Figure S8) [26]. While the carbonylic PCA/PDCAs fragments are upfield-shifted with respect to their corresponding free ligand (**L-1**–**L-5**) (Table 1) (e.g., $\delta_{C=O}$ = 167 (**1**) vs. 175 (**L-1**) ppm), with a downfield shift observed in the ^{31}P NMR spectra, upon complexation (e.g., δ_{P} = 29.8 (**1**) vs. −4.0 (**L-1**) ppm) (Figures S6–S15) [9,11,27–29]. Similar deshielding for the amide N*H* signals, is also observed in the ^{1}H NMR spectra of compounds **1**–**3** (e.g., δ_{H} = 8.63 (**1**) vs. 5.35 (**L-1**) ppm). This is most likely a consequence of intramolecular hydrogen bonding interactions upon introduction of the [Ru(*p*-cym)Cl_2] moiety (vide infra).

Table 1. Selected NMR spectroscopic data δ (ppm) for the free PCA/PDCAs **L-1**–**L-5**, and complexes **1**–**7**.

Compound	^{31}P Free PCA/PDCA Ligand [a]	^{31}P PCA/PDCA Complex [b]	$^{13}C\{^{1}H\}_{C=O}$ PCA/PDCA Complex [b]	$^{1}H_{NH}$ PCA/PDCA Complex [b]
1	−4.0	29.8 [a]	167.4 [a]	8.6 [a]
2	−0.2	37.2	167.6	10.1
3	−0.9	36.6	167.5	10.0
4	8.3	33.5	178.2/177.7 [c]	9.2
5	8.0	33.8	177.9/177.5 [c]	9.2
6	-	52.6	- [d]	-
7	-	52.3	170.9/162.1[c]	-

[a] Chemical shifts reported in ppm in C_6D_6. [b] Chemical shifts reported in ppm in CD_2Cl_2. [c] Chemical shifts for $Ph_2P_{(C=O)}$ and $N_{(C=O)}$ in ppm. [d] Signal not observed.

Crystals of compounds **1**–**5** suitable for single-crystal X-ray diffraction investigations were obtained from toluene solutions at room temperature (Figures 1 and S1–S5 and see the Supporting Information for additional crystallography details). In the solid-state, **1**–**5** feature a pseudo-octahedral geometry in a classical piano-stool arrangement, in which the coordination sphere consists of an η^6-bound *p*-cymene, two chloride ligands, and the P donor from the PCA/PDCA ligand (Figure 1). In the particular case of the structures of **4** and **5**, the core of the PDCA ligands is twisted compared to the free ligand, [9] which most likely arises from $\pi\cdots\pi$ stacking interactions between an aminic aryl group and the phenyl phosphine fragment, and highlights the conformational flexibility of the PDCA ligand [C17plane - C24plane = 3.545(2) Å (**4**); $C23_{plane}$ - $C9_{plane}$ = 3.540(2) Å (**5**)]. The Ru–Cl and Ru–P distances for **1**–**5** (Table 2), are similar to related phosphorus-bound ruthenium compounds [2,15,16,24,25,30] such as [Ru(*p*-cym){PH_2(CO)N*H*Cy}Cl_2] and [Ru(*p*-cym){$PPh_2C{\equiv}CPh$}Cl_2] (Ru–Cl; ≈ 2.40 Å, Ru–P; ≈ 2.35 Å) [2,24]. In the case of the crystal structure determinations for **1**, **4** and **5**, additional interstitial molecules of solvent were found (C_6H_6 and toluene, respectively) and could be sensibly modelled. In addition, complexes **1**–**5** present intramolecular hydrogen bonding between the amidic proton and one of the metal-bound chlorides in the solid state. Particularly, and due to the interaction between H1 and Cl1, the distances Ru1–Cl1 and Ru1–Cl2 are not equivalent; this is most noticeable in the determinations for **4** and **5** (Table 2).

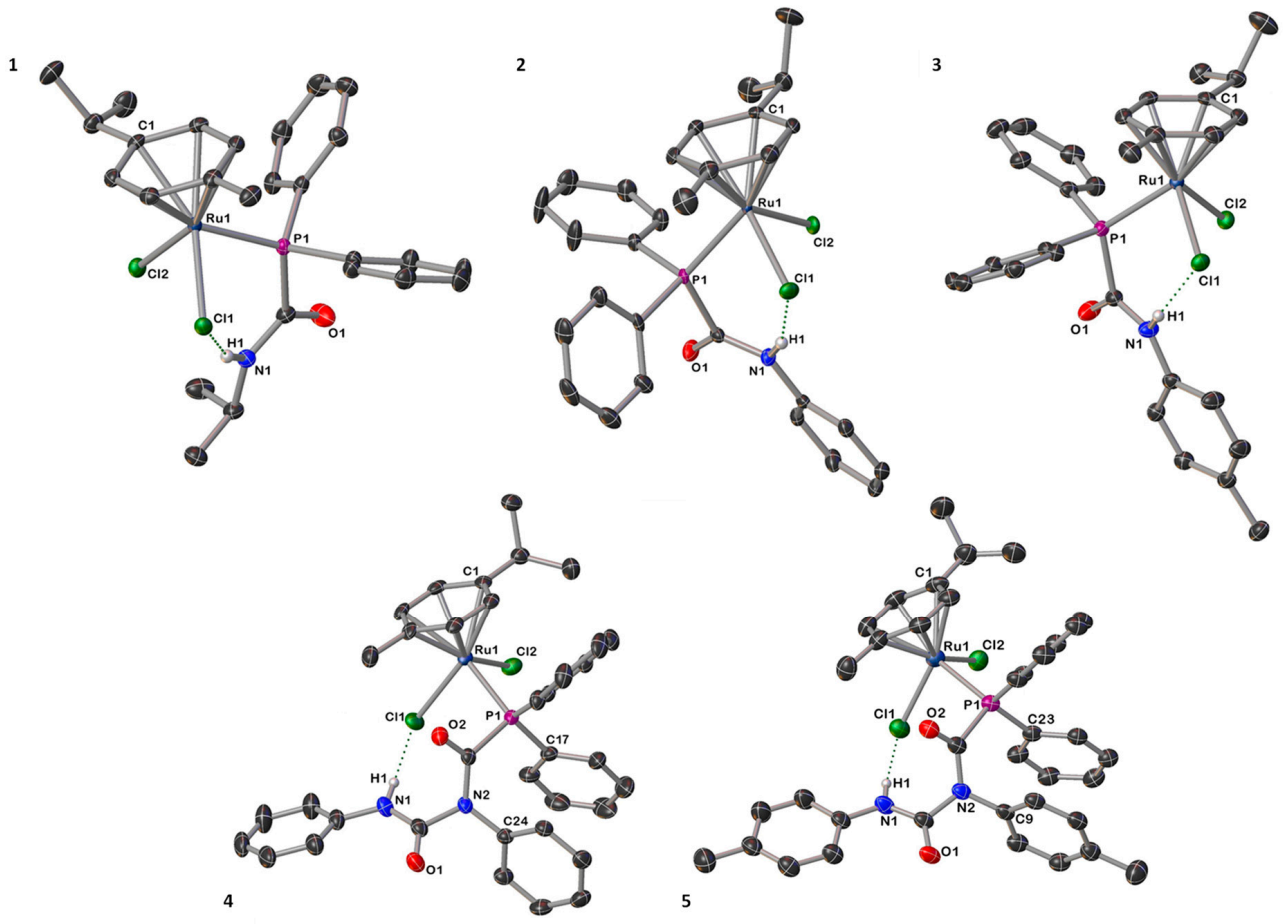

Figure 1. Molecular structures of PCA-coordinated compounds **1**–**3** (**above**) and PDCA-bound complexes **4**–**5** (**below**), with anisotropic displacement ellipsoids set at 50% probability. Solvent of crystallization and carbon-bound hydrogen atoms are omitted for clarity.

Table 2. Selected bond lengths (Å) and angles (°) for **1**–**5**.

	1	**2**	**3**	**4**	**5**
$C1_{plane}$–Ru1	1.7010 (8)	1.7007 (10)	1.6989 (7)	1.7010 (11)	1.702 (2)
Ru1–Cl1	2.4183 (5)	2.4142 (6)	2.4171 (4)	2.3941 (7)	2.4302 (11)
Ru1–Cl2	2.4115 (5)	2.4151 (6)	2.4078 (4)	2.4296 (9)	2.3974 (10)
Ru1–P1	2.3476 (5)	2.3448 (6)	2.3517 (4)	2.3678 (7)	2.3635 (10)
H1···Cl1	2.54 (3) [a]	2.3455 (6)	2.28 (2)	2.3723 (8)	2.44 (5)
Cl1–Ru1–P1	86.96 (2)	85.17 (2)	90.44 (2)	87.45 (3)	86.49 (4)
Cl2–Ru1–P1	87.35 (2)	86.87 (2)	83.29 (2)	89.33 (2)	89.70 (4)

[a] The distances H1···Cl1 and H1···Cl2 in **1** are very similar in length; H1···Cl2 2.53(3) Å.

*2.2. Synthesis and Characterization of [Ru(p-cym){κ²-P,N-PPh₂C(=O)N(R)C(=O)NR}Cl] ([R = Ph (**6**), p-tol (**7**)]*

With the intention to synthesize six-membered metallacycles via intramolecular cyclization, compounds **4** and **5** were reacted with K_2CO_3 and $AgPF_6$ in CD_2Cl_2 at room temperature (Scheme 2A), affording **6** and **7**, respectively (Figures S16–S22). In contrast, compound **2** showed no reaction under the same conditions. It is likely that the formation of the four-membered metallacycle is prohibited due to the higher ring strain resulting from the shorter PCA backbone.

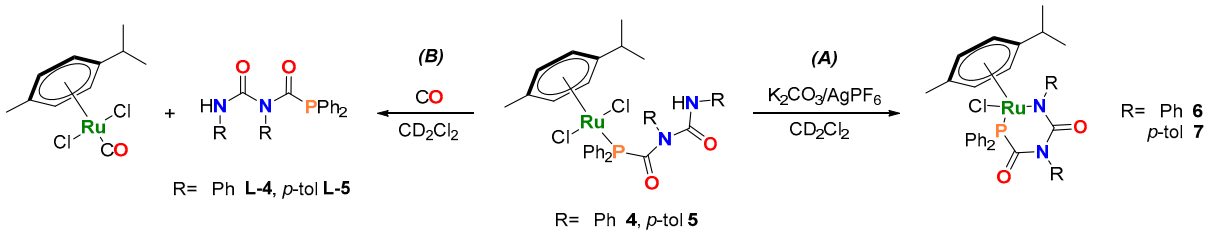

Scheme 2. (**A**) Formation of six-membered metallacycles (**6** and **7**). Reaction conditions: 1 eq. **4** or **5**, 3 eq. K_2CO_3 and 1.3 eq. $AgPF_6$, room temperature. (**B**) Ligand replacement reaction upon exposure to CO. Reaction conditions: 1 eq. of **4** or **5**, excess CO, room temperature.

The ^{31}P NMR spectroscopic resonances for the cyclized products **6** and **7** are shifted downfield with respect to the corresponding monodenate complexes **4** and **5** (Table 1). This is in line with previously reported six-membered *N*,*P*-metallacycles, such as [Ru-κ^3-*NNP*-{HCl(CO)}]; and [NNP = 3-(di-*tert*-butylphosphino)-*N*-[(1-methyl-1*H*-imidazol-2-yl)methyl]propylamine] (Figures S19 and S24) [27–29]. Our NMR spectroscopic studies support the structure described in Scheme 2 (Figures S17, S18, S21–S23 and S26–S28); and we propose that upon initial coordination (**6**–**7**), reaction with K_2CO_3 can deprotonate the PDCA amide. However, it is not until one of the coordinated halides is removed by $AgPF_6$, that formal cyclization takes place. This assertion has been corroborated by deprotonation experiments, in the absence of $AgPF_6$. Further halide replacement by $[PF_6]^-$ has been ruled out by means of NMR spectroscopy and MS analyses (ion trap). Although one resonance is observed in the ^{31}P NMR spectra (Table 1), both **6** and **7** are observed to exist as a mixture of two distinct isomers (**6a**–**7a**/**6b**–**7b**), as determined by ^{1}H NMR spectroscopy (Figures S16–S24 and Table S1). Additionally, ^{1}H-^{1}H COSY NMR spectra of the cyclized products (**6**–**7**), allowed for the deconvolution of the signals associated with the individual products, with distinctive correlations between the individual ^{i}Pr fragments (Figures S18 and S22). Integration of the ^{1}H NMR signals from the *p*-cymene ring indicate an isomer ratio of 60:40 for **6** and 87:13 for **7**. In both cases, the major product shows a complete loss of symmetry (as observed by ^{1}H and ^{13}C{^{1}H} NMR spectra) on the *p*-cymene fragment (Figures S18 and S22), with the minor product remaining bilaterally symmetrical (**6a**–**7a** (symmetric) and **6b**–**7b** (asymmetric)). The diffusion coefficients (D) of **2**, **5** and **7**, determined by DOSY NMR experiments (Table S1), allowed for the calculation of the hydrodynamic radii. These values are in good agreement with the values obtained from the crystal structures of **2** and **5**, and the geometry optimized structures of **7** (vide infra). An increase in the hydrodynamic radius is observed between **2** and **5** due to the increased length of the ligand, with only a small change in hydrodynamic radius observed upon cyclization (**7**). Similar to compounds **1**–**5**, scalar spin–spin coupling is observed in the ^{13}C{^{1}H} NMR spectra of **6** and **7** between the *p*-cymene and the phosphorus of the PDCA ligand [^{13}C{^{1}H} NMR] (Figure S22) [31]. With the signals for the non-quaternary aromatic carbons, in the *p*-cymene fragment, as four distinctive doublets ($^2J_{CP}$ = 3–6 Hz) (Figure S22).

The existence of two rotational isomers for compounds **6** and **7** can be explained by the restricted rotation of the *p*-cymene ring. DFT calculations demonstrate the existence of two rotamers, with either the ^{i}Pr (**6a′**/**7a′**) or Me (**6b′**/**7b′**) of the *p*-cymene ring lying above the Cl ligand (Figure 2 and Figures S26–S28). These rotamers are computed to be close in energy ($\Delta G = -0.4$ kcal mol^{-1} in **6** and -0.2 kcal mol^{-1} in **7**), suggesting minimal thermodynamic preference for either isomer. We propose, therefore, that the product distribution is determined by kinetic control. The strong preference for one isomer in **7** is likely due to a strong conformational preference for complex **5** in solution, which gets "locked in" when the complex cyclises on treatment with a halide abstractor and base. High-temperature NMR measurements on **6** and **7** were hindered as the complexes display poor solubility in $CD_3C_6D_5$ and decompose in $CDCl_3$ and CD_3CN. Variable temperature NMR studies (^{1}H and ^{31}P NMR spectroscopy) in CD_2Cl_2 (268–298 K) showed no coalescence, indicating higher temperatures are required for interconversion.

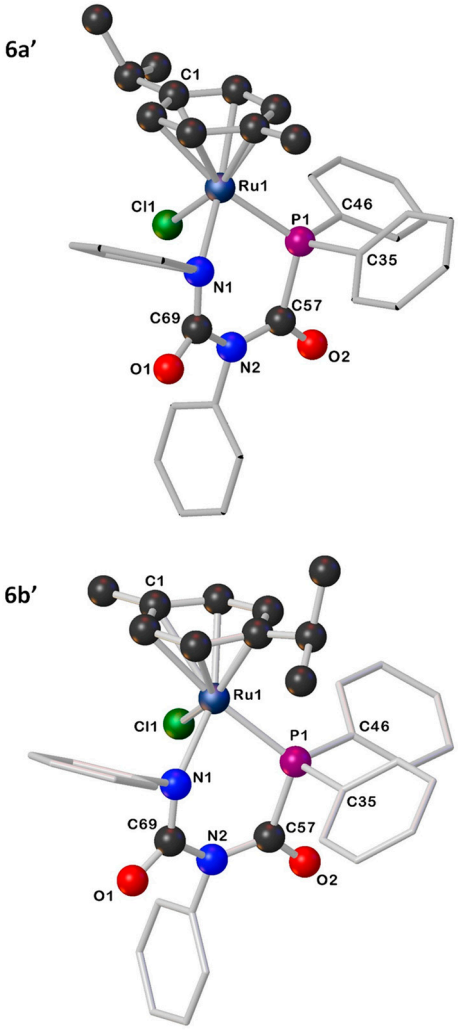

Figure 2. Illustrations for the geometry-optimized structures for **6a′** and **6b′**.

2.3. Ligand Displacement Studies

To test the stability of the Ru–P bond, solutions of **4** and **5** in CD_2Cl_2 were exposed to an atmosphere of dry CO (Scheme 2B). NMR analysis indicated loss of the PDCA ligands and formation of [{*p*-cymene}$RuCl_2$(CO)] [32] (Figure S25). Similar behaviour has been observed in [Rh(η^3-TMPP)$_2$][BF_4]$_2$ [TMPP = *tris*(2,4,6-trimethoxyphenyl)phosphine] that when exposed to an atmosphere of CO, can reversibly coordinate, a useful feature that has been used for chemosensing applications [33,34]. In contrast, no reaction was observed on treating the metallacycle **6** with CO, suggesting that the chelate complex is more robust to ligand substitution.

3. Materials and Methods

For full details on experimental procedures, see the Supporting Information.

Note: We observed that although compounds **1**–**3** display some stability, under aerobic conditions, decomposing over the course of a few weeks; samples of **4**–**7** are susceptible to spontaneous decomposition in solution/solid-state in the glovebox.

L-1–**L-5** were prepared according to our previously reported methodologies [9].

Crystals suitable for single-crystal X-ray diffraction for **1**–**5** were grown from concentrated toluene (layered with hexane) or C_6D_6 extracts at room temperature, respectively.

The phosphine (**L-1** 12 mg; **L-2** 6.9 mg; **L-3** 5.2 mg; **L-4** 6.9 mg; **L-5** 7.4 mg, 0.016 mmol) was dissolved in CD_2Cl_2 (0.4 mL) and added dropwise to a solution of [Ru(*p*-cymene)Cl_2]$_2$ (5 mg, 8.16×10^{-3} mmol) in CD_2Cl_2 (0.4 mL) with stirring, affording an orange solution.

Volatiles were removed under vacuum, affording the target compounds **1**–**5**. In the particular case of **2**, the reaction was successfully scaled up, employing 50 mg (0.08 mmol) of [Ru(*p*-cymene)Cl_2]$_2$, with full characterization described below. Figure 3 shows the general numbering scheme used for the the *p*-cymene ligand in compounds **1**–**5**.

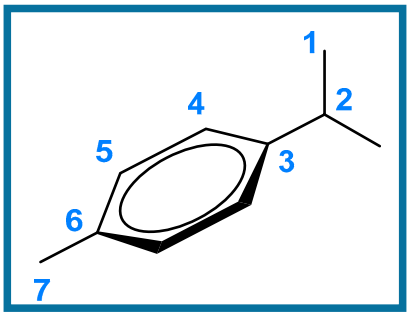

Figure 3. General numbering scheme for the *p*-cymene fragment for coordination compounds **1**–**5**.

[Ru(*p*-cym){$PPh_2C(=O)N(H)^iPr$}Cl_2] (**1**). ^{1}H NMR δ/ppm (400 MHz, C_6D_6): 8.63 (d, $^3J_{HP}$ = 7.4 Hz, 1H, N*H*), 8.20–8.02 (m, 4H, $PPh_2{}^o$), 7.14–6.94 (m, 6H, $PPh_2{}^{m+p}$), 4.75 (d, $^3J_{HH}$ = 6.1 Hz, 2H, *H*-5), 4.70 (dd, $^3J_{HH}$ = 6.1 Hz, $^3J_{HP}$ = 1.3 Hz, 2H, *H*-4), 4.05 (m, 1H, N^iPr^{CH}), 2.56 (sept, $^3J_{HH}$ = 7.0 Hz, 1H, *H*-2), 1.51 (s, 3H, *H*-7), 1.04 (d, $^1J_{HH}$ = 6.6 Hz, 6H, N^iPr^{CH3}), 0.82 (d, $^3J_{HH}$ = 7.0 Hz, 6H, *H*-1). $^{13}C\{^1H\}$ δ/ppm (400 MHz, C_6D_6): 167.4 (d, $^1J_{CP}$ = 55 Hz, C=O), 134.8 (d, $^2J_{CP}$ = 9 Hz, $PPh_2{}^o$), 133.7 (d, $^1J_{CP}$ = 43 Hz, $PPh_2{}^i$), 130.7 (d, $^4J_{CP}$ = 2 Hz, $PPh_2{}^p$), 128.2 (d, $^3J_{CP}$ = 10 Hz, $PPh_2{}^m$), 109.7 (C-6), 95.2 (C-3), 89.7 (d, $^2J_{CP}$ = 4 Hz, C-4), 86.0 (d, $^2J_{CP}$ = 6 Hz, C-5), 43.6 (d, *J* = 6 Hz, N^iPr^{CH}), 30.3 (C-2), 22.2 (C-1), 21.7 (N^iPr^{CH3}), 17.3 (C-7). ^{31}P NMR δ/ppm (162 MHz, C_6D_6): 29.8 (s, 1P, Ru*P*Ph_2). Anal. Calcd for $C_{26}H_{32}Cl_2NOPRu$: C 54.08, H 5.59, N 2.43; Found C 53.64, H 5.58, N 2.53. HRMS (ESI)$^+$ *m*/*z*: $[M+H]^+$ calculated 578.0715; found 578.0712 formula $C_{26}H_{33}Cl_2NOPRu$. IR (ATR) $\bar{\nu}_{max}$/cm^{-1}: 3237 (N-H), 1654 (C=O). Red crystalline solid, 5 mg, 39%.

[Ru(*p*-cym){$PPh_2C(=O)N(H)Ph$}Cl_2] (**2**). ^{1}H NMR δ/ppm (400 MHz, CD_2Cl_2): 10.11 (s, 1H, N*H*), 7.88 (ddd, $^3J_{HH}$ = 10.0 Hz, $^3J_{HH}$ = 8.2 Hz, $^3J_{HH}$ = 1.4 Hz, 4H, $PPh_2{}^m$), 7.5–7.47 (m, 4H, $PPh_2{}^o$), 7.44 (d, $^3J_{HH}$ = 8.4 Hz, 2H, NPh^o), 7.42–7.38 (m, 2H, $PPh_2{}^p$), 7.21 (t, J = 7.6 Hz, 2H, NPh^m), 7.02 (t, $^3J_{HH}$ = 7.4 Hz, 1H, NPh^p), 5.29 (d, $^3J_{HH}$ = 6.4 Hz, 2H, *H*-5), 5.27 (d, $^3J_{HH}$ = 6.3 Hz, 2H, *H*-4), 2.55 (sept, $^3J_{HH}$ = 7.0 Hz, 1H, *H*-2), 1.84 (s, 3H, *H*-7), 1.04 (d, $^3J_{HH}$ = 7.0 Hz, 6H, *H*-1). $^{13}C\{^1H\}$ NMR δ/ppm (100 MHz, CD_2Cl_2): 167.8 (d, $^1J_{CP}$ = 55 Hz, C=O), 137.0 (NPh^i), 134.7(d, $^3J_{CP}$ = 9 Hz, $PPh_2{}^m$), 131.8 (d, $^3J_{CP}$ = 2 Hz, $PPh_2{}^o$), 129.9 ($PPh_2{}^i$), 129.3 (NPh^m), 129.1(d, $^2J_{CP}$ = 7 Hz, $PPh_2{}^p$), 124.9 (NPh^p), 120.3 (NPh^o), 111.0 (C-6), 97.3 (C-3), 90.1 (d, $^2J_{CP}$ = 4 Hz, C-4), 86.9 (d, $^2J_{CP}$ = 5 Hz, C-5), 30.9 (C-2), 22.1 (C-1), 17.9 (C-7). ^{31}P NMR δ/ppm (162 MHz, CD_2Cl_2): 37.2 (s, 1P, Ru*P*Ph_2). Anal. Calcd for $C_{29}H_{30}Cl_2NOPRu$: C 56.96, H 4.95, N 2.29; Found C 55.48, H 5.01, N 2.30. HRMS/ESI$^+$ *m*/*z*: $[M+Na]^+$ calculated 634.0383; found 634.0387 formula $C_{29}H_{30}Cl_2NNaOPRu$. IR (ATR) $\bar{\nu}_{max}$/cm^{-1}: 3227 (N-H), 1655 (C=O). Dark red powder, 53 mg, 51%.

[Ru(*p*-cym){$PPh_2C(=O)N(H)p$-tol}Cl_2] (**3**). ^{1}H NMR δ/ppm (400 MHz, CD_2Cl_2): 10.03 (s, 1H, N*H*), 7.90–7.84 (m, 4H, $PPh_2{}^o$), 7.57–7.47 (m, 6H, $PPh_2{}^{m+p}$), 7.32 (d, $^3J_{HH}$ = 8.4 Hz, 2H, NPh^m), 7.01 (d, $^3J_{HH}$ = 8.2 Hz, 2H, NPh^o), 5.28 (d, $^3J_{HH}$ = 6.9 Hz, 2H, *H*-5), 5.26 (d, $^3J_{HH}$ = 6.7 Hz, 2H, *H*-4), 2.53 (sept, $^3J_{HH}$ = 6.9 Hz, 1H, *H*-2), 2.24 (s, 3H, $NPh^{CH}{}_3{}^i$), 1.83 (s, 3H, *H*-7), 1.03 (d, $^3J_{HH}$ = 7.0 Hz, 6H, *H*-1). $^{13}C\{^1H\}$ NMR δ/ppm (100 MHz, CD_2Cl_2): 167.5 (C=O), 136.2 ($NPh^{CH}{}_3{}^i$), 134.7 ($PPh_2{}^o$), 134.6 (NPh^i), 131.8 (d, $^4J_{CP}$ = 2 Hz, $PPh_2{}^p$), 129.7 (NPh^o), 128.9 (d, $^3J_{CP}$ = 10 Hz, $PPh_2{}^m$), 120.2 (NPh^m), 110.9 (C-6), 97.2 (C-3), 90.1 (d, $^2J_{CP}$ = 4 Hz, C-4), 86.9 (d, $^2J_{CP}$ = 5 Hz, C-5), 81.4 (d, $^1J_{CP}$ = 70 Hz, $PPh_2{}^i$), 30.8 (C-2), 22.1 (C-1), 21.1 ($NPh^{CH}{}_3$), 17.9 (C-7). ^{31}P NMR δ/ppm (162 MHz, CD_2Cl_2): 36.6 (s, 1P, Ru*P*Ph_2). Anal. Calcd for $C_{30}H_{32}Cl_2NOPRu$: C 57.60, H 5.16, N 2.24; Found C 56.86, H 5.21, N 2.22. HRMS/ESI$^+$ *m*/*z*: $[M-Cl]^+$ calculated 590.0948, found 590.0961 formula $C_{30}H_{32}ClNOPRu$. IR (ATR) $\bar{\nu}_{max}$/cm^{-1}: 3180 (N-H), 1665 (C=O). Dark red powder, Quantitative yield, 11 mg.

[Ru(*p*-cym){$PPh_2C(=O)N(Ph)C(=O)N(H)Ph$}$Cl_2$] (**4**). ^{1}H NMR δ/ppm (400 MHz, CD_2Cl_2): 9.25 (s, 1H, N*H*), 7.71 (t, 3H, J = 9.0 Hz, *H*-ArP), 7.54–7.49 (dd, J = 11.8, 7.1 Hz, 2H, *H*-ArN), 7.42–7.37 (m, 3H, *H*-ArN), 7.33–7.30 (m, 2H, *H*-ArP), 7.26–7.05 (m, 9H, *H*-ArN/*H*-ArP), 6.98 (d, J = 7.4 Hz, 1H, *H*-ArN), 5.45 (d, $^3J_{HH}$ = 6.0 Hz, 2H, *H*-4), 5.15 (d, $^3J_{HH}$ = 6.0 Hz, 2H, *H*-5), 2.69 (sept, $^3J_{HH}$ = 6.7 Hz, 1H, *H*-2), 1.91 (s, 1H, *H*-7), 1.11 (d, $^3J_{HH}$ = 6.9 Hz, 2H, *H*-1). $^{13}C\{^1H\}$ NMR δ/ppm (100 MHz, CD_2Cl_2): 178.1 (C=O), 177.7 (C=O), 138.2 (d, $^1J_{CP}$ = 9 Hz, PPh_2^i), 134.9 (d, J = 9 Hz, ArP), 131.3 (d, J = 2.5 Hz, ArP), 129.9 (ArN), 129.8 (ArN), 129.1, 128.7 (NPh^i *x2*), 128.6 (ArN), 128.3 (d, J = 10.1 Hz, ArP), 124.7 (ArN), 120.7 (ArN), 120.1 ArN), 110.2 (C-6), 96.9 (C-3), 92.1 (d, $^2J_{CP}$ = 4 Hz, C-4), 86.5 (d, $^2J_{CP}$ = 5 Hz, C-5), 30.7 (C-2), 22.3 (C-1), 17.5 (C-7). ^{31}P NMR δ/ppm (162 MHz, CD_2Cl_2): 33.50 (s, 1P, Ru*P*Ph_2). Anal. Calcd for $C_{36}H_{35}Cl_2N_2O_2PRu$: C 59.18, H 4.83, N 3.83; Found C 56.48, H 4.73, N 3.67. Despite repeated attempts, a satisfactory elemental analysis for this compound could not be obtained; derived from the aforementioned spontaneous decomposition. HRMS/ESI$^+$ m/z: [M-Cl]$^+$ calculated 695.1168, found 695.1158; formula $C_{36}H_{35}ClN_2O_2PRu$. Quantitative conversion as determined by ^{1}H NMR spectroscopy using TMS as internal standard.

[Ru(*p*-cym){$PPh_2C(=O)N(p\text{-tol})C(=O)N(H)p\text{-tol}$}$Cl_2$] (**5**). ^{1}H NMR δ/ppm (400 MHz, CD_2Cl_2): 9.20 (s, 1H, NH), 7.68 (t, $^3J_{HH}$ = 9.2 Hz, 4H, PPh_2^m), 7.34–7.30 (m, 4H, PPh_2^p), 7.25 (d, $^3J_{HH}$ = 8.5 Hz, 2H, N*H*Ph^m), 7.19 (td, $^3J_{HH}$ = 7.8, $^3J_{HH}$ = 2.0 Hz, 4H, PPh_2^o), 7.05 (d, $^3J_{HH}$ = 8.3 Hz, 2H, N*H*Ph^o), 6.88 (d, $^3J_{HH}$ = 8.2 Hz, 2H, NPh^o), 6.83 (d, $^3J_{HH}$ = 8.4 Hz, 2H, NPh^m), 5.44 (d, $^3J_{HH}$ = 5.4 Hz, 2H, H-4), 5.17 (d, $^3J_{HH}$ = 6.2 Hz, 2H, H-5), 2.70 (sept, $^3J_{HH}$ = 7.0 Hz, 1H, H-2), 2.29 (s, 3H, N*H*Ph^{CH_3}), 2.24 (s, 3H, NPh^{CH_3}), 1.90 (s, 3H, H-7), 1.11 (d, $^3J_{HH}$ = 7.0 Hz, 6H, H-1). $^{13}C\{^1H\}$ NMR δ/ppm (100 MHz, CD_2Cl_2):177.9 (C=O), 177.5 (C=O), 151.8 (PPh_2^i), 138.9 (NPh^i), 135.7 (N*H*$Ph^{CH_3}{}^i$), 135.2 ($NPh^{CH_3}{}^i$), 135.0 (d, $^3J_{CP}$ = 9 Hz, PPh_2^m), 134.5 (N*H*Ph^i), 131.1 (d, $^4J_{CP}$ = 3 Hz, PPh_2^p), 130.4 (NPh^o) 129.7 (N*H*Ph^o), 128.6 (NPh^m), 128.2 (d, $^2J_{CP}$ = 10 Hz, PPh_2^o), 120.0 (N*H*Ph^m), 110.1 (C-6), 96.9 (C-3), 92.1 (d, $^2J_{CP}$ = 4 Hz, C-4), 86.5 (d, $^2J_{CP}$ = 6 Hz, C-5), 30.8 (C-2), 22.3 (C-1), 21.3 (NPh^{CH_3}), 21.1 (N*H*Ph^{CH_3}), 17.45 (C-7). ^{31}P NMR δ/ppm (162 MHz, CD_2Cl_2): 33.76 (s, 1P, Ru*P*Ph_2). Anal. Calcd for $C_{38}H_{39}Cl_2N_2O_2PRu$: C 60.16, H 5.18, N 3.69; Found C 60.12, H 5.43, N 3.20. HRMS/ESI$^+$ m/z: [M-Cl]$^+$ calculated 723.1476, found 723.1489; formula $C_{38}H_{39}ClN_2O_2PRu$. Quantitative conversion by NMR using TMS as internal standard. Dark red/orange powder, 15 mg.

Typical procedure for the formation of metallacycles **6** and **7**. A solution containing **4** or **5** (0.016 mmol) in CD_2Cl_2 (0.6 mL) was added to a mixture of K_2CO_3 (6.8 mg, 0.048 mmol) and $AgPF_6$ (5.4 mg, 0.02 mmol) (as solids), and transferred to a J. Young's tap NMR tube. The heterogeneous mixture was agitated via sonication at room temperature for 10 min, and filtered, affording an orange-red solution. Removal of volatiles in vacuo afforded full conversion to the cyclized products **6** and **7**, respectively. Quantitative conversion was determined by ^{1}H NMR spectroscopy using TMS as the internal standard. Figure 4 shows the general numbering scheme used for the the *p*-cymene ligand in compounds **6** and **7**.

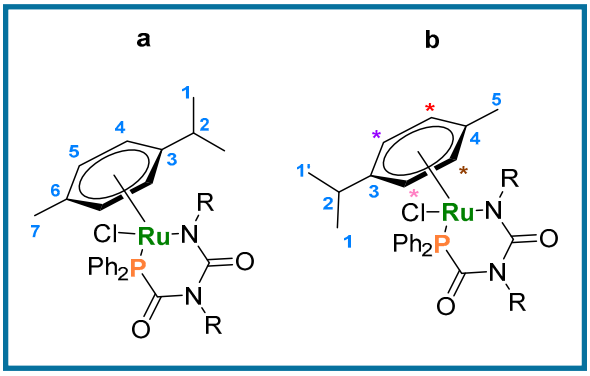

Figure 4. General numbering scheme for cyclization compounds **6a** and **b** (R = Ph) and **7a** and **b** (R= *p*-tol). * indicate multiplets in the NMR spectrum.

[Ru(*p*-cym){κ^2-*P,N*-$PPh_2C(=O)N(Ph)C(=O)NPh$}Cl] (**6**). Mixture of 2 products, ratio 60:40. (**6b** as main product) Characterization for **6a** and **6b**: ^{1}H NMR δ/ppm (400 MHz, CD_2Cl_2): 7.81–7.71 (m, Ph), 7.66–7.63 (m, 2H, Ph), 7.58–7.53 (m, Ph), 7.51 (d, J = 7.7 Hz, 6H, NPh), 7.47–7.37 (m, Ph), 7.23 (d, J = 7.6 Hz, 4H, NPh), 7.03 (s, 2H, Ph), 5.69–5.62 (m, 4H, **6b**-^{i}Pr-C_6H_4-Me), 5.64 (d, $^3J_{HH}$ = 6.1 Hz, 2H, **6a**-H5), 5.46 (d, $^3J_{HH}$ = 6.1 Hz, 2H, **6a**-H4), 2.78 (sept, J = 6.8 Hz, 1H, **6a**-H2), 2.21 (s, 3H, **6a**-H7), 1.85 (sept, J = 6.86 Hz, 1H, **6b**-H2), 1.64 (s, 3H, **6b**-H5), 1.30 (d, J = 6.9 Hz, 6H, **6a**-H1), 0.83 (d, $^3J_{HH}$ = 6.9 Hz, 3H, **6b**-H1), 0.78 (d, $^3J_{HH}$ = 6.9 Hz, 3H, **6b**-H1′). ^{13}C{^{1}H} NMR δ/ppm (100 MHz, CD_2Cl_2): 135.4 (d, J = 11 Hz, Ph), 134.3 (d, J = 36 Hz, Ph), 133.9 (d, J = 2 Hz, Ph), 133.7 (d, J = 10.1 Hz, Ph), 131.7 (d, J = 20 Hz, Ph), 130.9 (d, J = 10 Hz, Ph), 130.1 (NPh), 129.4 (d, J = 11 Hz, Ph), 129.2 (d, J = 11 Hz, Ph), 126.5 (NPh), 108.8 (**6b**-C4), 102.4 (**6a**-C6), 97.7 (**6a**-C3), 97.3 (**6b**-C3), 90.5 (d, $^2J_{CP}$ = 3 Hz, **6b**-^{i}Pr-C_6H_4-Me), 88.3 (d, $^2J_{CP}$ = 6 Hz, **6b**-^{i}Pr-C_6H_4-Me), 87.2 (d, $^2J_{CP}$ = 3 Hz, **6b**-^{i}Pr-C_6H_4-Me), 85.6 (d, $^2J_{CP}$ = 4 Hz, **6b**-^{i}Pr-C_6H_4-Me), 79.4 (**6a**-C5), 78.6 (**6a**-C4), 31.9 (**6a**/**6b**-C2), 22.2 (**6b**-C1), 21.4 (**6a**-C1), 20.9 (**6b**-C1′), 19.3 (**6a**-C7), 17.9 (**6b**-C5). ^{31}P NMR δ/ppm (162 MHz, CD_2Cl_2): 52.59 (s, 1P, RuPPh$_2$). HRMS/ESI$^+$ m/z: $[M+H]^+$ calculated 695.1168, found 695.1175; formula $C_{36}H_{35}ClN_2O_2PRu$. IR (ATR) $\bar{\upsilon}_{max}$/cm^{-1}: 1616 (C=O), 1584 (C=O). Dark orange powder, 10 mg, 88%.

[Ru(*p*-cym){κ^2-*P,N* $PPh_2C(=O)N(p\text{-tol})C(=O)N$*p*-tol}Cl] (**7**). Mixture of 2 products, ratio 87:13. (**7b** as main product). Characterization for **7b**: ^{1}H NMR δ/ppm (400 MHz, CD_2Cl_2): 7.80–7.70 (m, 7H, *H*-ArP), 7.64 (tq, J = 7.5, 2.04 Hz, 1H, *H*-ArP), 7.53 (td, J = 7.6, 3.0 Hz, 2H, *H*-ArP), 7.33 (t, $^3J_{HH}$ = 8.1 Hz, 5H, *H*-ArN), 7.10 (d, $^3J_{HH}$ = 8.3 Hz, 3H, *H*-ArN), 5.64-5.69 (m, 3H, ^{i}Pr-C_6H_4-Me), 5.62 (d, $^3J_{HH}$ = 6.3 Hz, 1H, ^{i}Pr-C_6H_4-Me), 2.42 (s, 3H, *H*6), 2.39 (s, 3H, *H*7), 1.85 (sept, $^3J_{HH}$ = 6.9 Hz, 1H, *H*2), 1.65 (s, 3H, *H*5), 0.84 (d, $^3J_{HH}$ = 7.0 Hz, 3H, *H*1), 0.79 (d, $^3J_{HH}$ = 7.0 Hz, 3H, *H*1′). ^{13}C{^{1}H} NMR δ/ppm (100 MHz, CD_2Cl_2): 170.9 (d, $^1J_{CP}$ = 51 Hz, Ph_2P-C=O), 162.1 (d, $^3J_{CP}$ = 3 Hz, C=O), 142.5 (quat-N), 139.6 (quat-N), 135.4 (d, J = 11 Hz, ArP), 133.8 (d, J = 3 Hz, ArP), 133.6 (d, J = 10 Hz, ArP), 132.2 (quat-N), 131.4 (ArN), 130.8 (d, J = 10 Hz, ArP), 130.5 (quat-N), 129.4 (d, J = 11 Hz, ArP), 127.1 (d, J = 45 Hz, ipso-P), 126.3 (d, J = 51 Hz, ipso-P), 126.2 (ArN), 108.8 (d, $^2J_{CP}$ = 2 Hz, C4), 97.1 (C3), 90.6 (d, $^2J_{CP}$ = 4 Hz, ^{i}Pr-C_6H_4-Me), 88.1 (d, $^2J_{CP}$ = 6 Hz, ^{i}Pr-C_6H_4-Me), 87.1 (d, $^2J_{CP}$ = 2 Hz, ^{i}Pr-C_6H_4-Me), 85.6 (d, $^2J_{CP}$ = 4 Hz, ^{i}Pr-C_6H_4-Me), 31.1 (C2), 22.1 (C1), 21.5 (C7), 21.4 (C-6), 20.8 (C1′), 17.9 (C5). ^{31}P NMR δ/ppm (162 MHz, CD_2Cl_2): 52.34 (s, 1P, RuPPh$_2$). HRMS/ESI$^+$ m/z: $[M+H]^+$ calculated 723.1476, found 723.1477; formula $C_{38}H_{39}ClN_2O_2PRu$. IR (ATR) $\bar{\upsilon}_{max}$/cm^{-1}: 1594 (C=O), 1509 (C=O). Dark orange powder, 10 mg, 85%.

Typical procedure for reactivity with CO. An NMR tube containing a solution of **4** (0.016 mmol) in 0.6 mL of CD_2Cl_2, was charged with an atmosphere of CO via three freeze–thaw cycles. The resulting sample was studied via multinuclear NMR spectroscopies (^{1}H, ^{13}C{^{1}H} and ^{31}P NMR); showing formation of the corresponding free phosphine/PDCA (**L-4**) and [{*p*-cymene}$RuCl_2$(CO)], in accordance with the reported literature [9,32].

4. Conclusions

We have described the synthesis of ruthenium(II) complexes coordinated by PCAs and PDCAs, and the first reports of PDCAs as both monodentate and bidentate ligands. In the case of the metallacycles **6** and **7** a mixture of two isomers is obtained, as evidenced by NMR spectroscopy. Whilst the monodentate coordination motif in these complexes can be displaced by CO, chelates **6** and **7** are robust to ligand displacement reactions.

Supplementary Materials: The following supporting information can be downloaded at: https://www.mdpi.com/article/10.3390/inorganics11090372/s1, The Electronic Supplementary Information (ESI) available is as follows: full experimental details for the synthesis, characterization, and analysis (References [9,35–46] are cited in the Supplementary Materials).

Author Contributions: Conceptualization: A.M.G. and D.L.K.; Methodology, R.N.-S., A.M.G., H.R.S., L.J.T. and D.L.K.; Investigation R.N.-S., A.M.G., H.R.S., T.G.L.-W., A.J. and J.A.; Formal analysis, R.N.-S., A.M.G., H.R.S., T.G.L.-W., A.J., J.A., L.J.T., J.M., W.L., A.J.B. and D.L.K.; Resources, C.D.H.; Visualization, R.N.-S., A.M.G., L.J.T. and D.L.K.; Data curation, R.N.-S., A.M.G. and D.L.K.; Writing—original draft, R.N.-S. and A.M.G.; Writing—review and editing, R.N.-S., A.M.G., L.J.T., A.J.B., W.L., J.M. and D.L.K.; Supervision, J.M. and D.L.K.; Project administration, D.L.K.; Funding acquisition, R.N.-S. and D.L.K. All authors have read and agreed to the published version of the manuscript.

Funding: This research was funded by the Engineering and Physical Sciences Research Council (grant numbers EP/R004064/1; EP/L015633/1); The Leverhulme Trust (grant number RPG-2014-317); CONACYT (Mexican Council for Science and Technology) (grant number CVU 600474) and the University of Nottingham.

Data Availability Statement: A dataset supporting this research can be found at https://doi.org/10.17639/nott.7265. CCDC 1935805-1935809 contain the supplementary crystallographic data for this article. These data can be obtained free of charge from The Cambridge Crystallographic Data Centre via www.ccdc.cam.ac.uk/structures.

Acknowledgments: We thank the EPSRC UK National Mass Spectrometry Facility at Swansea University and University of Nottingham facilities for mass spectrometry.

Conflicts of Interest: The authors declare no conflict of interest.

References

1. Štěpnička, P. Phosphino-Carboxamides: The Inconspicuous Gems. *Chem. Soc. Rev.* **2012**, *41*, 4273–4305. [CrossRef] [PubMed]
2. Jupp, A.R.; Trott, G.; Payen De La Garanderie, É.; Holl, J.D.G.; Carmichael, D.; Goicoechea, J.M. Exploiting the Brønsted Acidity of Phosphinecarboxamides for the Synthesis of New Phosphides and Phosphines. *Chem. Eur. J.* **2015**, *21*, 8015–8018. [CrossRef] [PubMed]
3. Jupp, A.R.; Goicoechea, J.M. Phosphinecarboxamide: A Phosphorus-Containing Analogue of Urea and Stable Primary Phosphine. *J. Am. Chem. Soc.* **2013**, *135*, 19131–19134. [CrossRef] [PubMed]
4. Fernandes, C.; Correia, J.D.G.; Gano, L.; Santos, I.; Seifert, S.; Syhre, R.; Bergmann, R.; Spies, H. Dramatic Effect of the Tridentate Ligand on the Stability of ^{99m}Tc "3 + 1" Oxo Complexes Bearing Arylpiperazine Derivatives. *Bioconjug. Chem.* **2005**, *16*, 660–668. [CrossRef]
5. Meléndez-Alafort, L.; Nadali, A.; Pasut, G.; Zangoni, E.; De Caro, R.; Cariolato, L.; Giron, M.C.; Castagliuolo, I.; Veronese, F.M.; Mazzi, U. Detection of Sites of Infection in Mice Using ^{99m}Tc-Labeled PN_2S-PEG Conjugated to UBI and ^{99m}Tc-UBI: A Comparative Biodistribution Study. *Nucl. Med. Biol.* **2009**, *36*, 57–64. [CrossRef]
6. Léautey, M.; Jubault, P.; Pannecoucke, X.; Quirion, J.C. Synthesis and Evaluation of a Broad Range of New Chiral (Aminoalkyl)Phosphane Ligands for Asymmetric Hydrogen-Transfer Reduction of Prochiral Ketones. *Eur. J. Org. Chem.* **2003**, *19*, 3761–3768. [CrossRef]
7. Sladojevich, F.; Trabocchi, A.; Guarna, A.; Dixon, D.J. A New Family of Cinchona-Derived Amino Phosphine Precatalysts: Application to the Highly Enantio- and Diastereoselective Silver-Catalyzed Isocyanoacetate Aldol Reaction. *J. Am. Chem. Soc.* **2011**, *133*, 1710–1713. [CrossRef]
8. Seidenkranz, D.T.; McGrath, J.M.; Zakharov, L.N.; Pluth, M.D. Supramolecular Bidentate Phosphine Ligand Scaffolds from Deconstructed Hamilton Receptors. *Chem. Commun.* **2017**, *53*, 561–564. [CrossRef]
9. Sharpe, H.R.; Geer, A.M.; Lewis, W.; Blake, A.J.; Kays, D.L. Iron(II)-Catalyzed Hydrophosphination of Isocyanates. *Angew. Chem. Int. Ed.* **2017**, *56*, 4845–4848. [CrossRef]
10. Braunstein, P.; Naud, F. Hemilability of Hybrid Ligands and the Coordination Chemistry of Oxazoline-Based Systems. *Angew. Chem. Int. Ed.* **2001**, *40*, 680–699. [CrossRef]
11. Geeson, M.B.; Jupp, A.R.; McGrady, J.E.; Goicoechea, J.M. On the Coordination Chemistry of Phosphinecarboxamide: Assessing Ligand Basicity. *Chem. Commun.* **2014**, *50*, 12281–12284. [CrossRef] [PubMed]
12. Sun, Y.; Zhang, Z.; Wang, X.; Li, X.; Weng, L.; Zhou, X. Isocyanate Diinsertion into the N-H Bond of the 2-Pyridylamino Ligand of Organolanthanides. *Dalton Trans.* **2010**, *39*, 221–226. [CrossRef] [PubMed]
13. Ito, M.; Iseki, M.; Itazaki, M.; Nakazawa, H. Tetrahedral Cage Complex with Planar Vertices: Selective Synthesis of Pt_4L_6 Cage Complexes Involving Hydrogen Bonds Driven by Halide Binding. *Chem. Commun.* **2016**, *52*, 7205–7208. [CrossRef] [PubMed]
14. Ding, F.; Sun, Y.; Verpoort, F. O,N-Bidentate Ruthenium Azo Complexes as Catalysts for Olefin Isomerization Reactions. *Eur. J. Inorg. Chem.* **2010**, *10*, 1536–1543. [CrossRef]
15. Rath, R.K.; Nethaji, M.; Chakravarty, A.R. Synthesis, Crystal Structure and Catalytic Properties of (*p*-cymene)Ruthenium(II) Azophenol Complexes: Azophenyl to Azophenol Conversion by Oxygen Insertion to a Ruthenium-Carbon Bond. *J. Organomet. Chem.* **2001**, *633*, 79–84. [CrossRef]

16. Rath, R.K.; Nethaji, M.; Chakravarty, A.R. Transfer Hydrogenation of Acetophenone Promoted by (Arene)Ruthenium(II) Reduced Schiff Base Complexes: An X-Ray Structure of [(η^6-*p*-cymene)RuCl(OC_6H_4-2-$CH_2NHC_6H_4$-*p*-Me)]. *Polyhedron* **2001**, *20*, 2735–2739. [CrossRef]
17. Bozec, H.; Le Touchard, D.; Dixneuf, P.H. Organometallic Chemistry of Arene Ruthenium and Osmium Complexes. *Adv. Organomet. Chem.* **1989**, *29*, 163–247.
18. Noyori, R.; Hashiguchi, S. Asymmetric Transfer Hydrogenation Catalyzed by Chiral Ruthenium Complexes. *Acc. Chem. Res.* **1997**, *30*, 97–102. [CrossRef]
19. Naota, T.; Takaya, H.; Murahashi, S.I. Ruthenium-Catalyzed Reactions for Organic Synthesis. *Chem. Rev.* **1998**, *98*, 2599–2660. [CrossRef] [PubMed]
20. Bruneau, C.; Dixneuf, P.H. Metal Vinylidenes in Catalysis. *Acc. Chem. Res.* **1999**, *32*, 311–323. [CrossRef]
21. Cadierno, V.; Gamasa, M.P.; Gimeno, J. Recent Developments in the Reactivity of Allenylidene and Cumulenylidene Complexes. *Eur. J. Inorg. Chem.* **2001**, *3*, 571–591. [CrossRef]
22. Bruce, M.I. Transition Metal Complexes Containing Allenylidene, Cumulenylidene, and Related Ligands. *Chem. Rev.* **1998**, *98*, 2797–2858. [CrossRef] [PubMed]
23. Touchard, D.; Dixneuf, P.H. A New Class of Carbon-Rich Organometallics. The C_3, C_4 and C_5 Metallacumulenes Ru=$(C=)_nCR_2$. *Coord. Chem. Rev.* **1998**, *178*, 409–429. [CrossRef]
24. Berenguer, J.R.; Bernechea, M.; Forniés, J.; García, A.; Lalinde, E. (*p*-cymene) Ruthenium (II) (Diphenylphosphino) Alkyne Complexes: Preparation of (μ-Cl) (μ-$PPh_2C{\equiv}CR$)-Bridged Ru/Pt Heterobimetallic Complexes. *Organometallics* **2004**, *23*, 4288–4300. [CrossRef]
25. Çalık, H.S.; Ispir, E.; Karabuga, Ş.; Aslantas, M. Ruthenium (II) Complexes of NO Ligands: Synthesis, Characterization and Application in Transfer Hydrogenation of Carbonyl Compounds. *J. Organomet. Chem.* **2016**, *801*, 122–129. [CrossRef]
26. Batsanov, S.S. Van Der Waals Radii of Elements. *Inorg. Mater.* **2001**, *37*, 871–885. [CrossRef]
27. Cabrero-Antonino, J.R.; Alberico, E.; Drexler, H.J.; Baumann, W.; Junge, K.; Junge, H.; Beller, M. Efficient Base-Free Hydrogenation of Amides to Alcohols and Amines Catalyzed by Well-Defined Pincer Imidazolyl-Ruthenium Complexes. *ACS Catal.* **2016**, *6*, 47–54. [CrossRef]
28. Adam, R.; Alberico, E.; Baumann, W.; Drexler, H.J.; Jackstell, R.; Junge, H.; Beller, M. NNP-Type Pincer Imidazolylphosphine Ruthenium Complexes: Efficient Base-Free Hydrogenation of Aromatic and Aliphatic Nitriles under Mild Conditions. *Chem. Eur. J.* **2016**, *22*, 4991–5002. [CrossRef]
29. Lee, C.C.; Huang, H.C.; Liu, S.T.; Liu, Y.H.; Peng, S.M.; Chen, J.T. Coordination Chemistry and Catalytic Activity of Ruthenium(II) Complexes Containing a Phospha-Macrocyclic Ligand. *Polyhedron* **2013**, *52*, 1024–1029. [CrossRef]
30. García de la Arada, I.; Díez, J.; Gamasa, P.; Lastra, E. Isomerization Processes on Organoruthenium Complexes Bearing κ^2(P,C)-Bidentate Ligands Generated Through Nucleophilic Addition To Coordinated Alkenyl Phosphanes. *Eur. J. Inorg. Chem.* **2018**, *45*, 4875–4886. [CrossRef]
31. Hierso, J.C. Indirect Nonbonded Nuclear Spin-Spin Coupling: A Guide for the Recognition and Understanding of "through-Space" NMR J Constants in Small Organic, Organometallic, and Coordination Compounds. *Chem. Rev.* **2014**, *114*, 4838–4867. [CrossRef] [PubMed]
32. Hodson, E.; Simpson, S.J. Synthesis and Characterisation of [(η^6-cymene)Ru(L)X_2] Compounds: Single Crystal X-ray Structure of [(η^6- cymene)Ru(P{OPh}$_3$)Cl_2] at 203 K. *Polyhedron* **2004**, *23*, 2695–2707. [CrossRef]
33. Dulebohn, J.I.; Berglund, K.A.; Haefner, S.C.; Dunbar, K.R. Reversible Carbon Monoxide Addition to Sol-Gel Derived Composite Films Containing a Cationic Rhodium(I) Complex: Towards the Development of a New Class of Molecule-Basedcarbon Monoxide Sensors. *Chem. Mater.* **1992**, *4*, 506–508. [CrossRef]
34. Dunbar, K.R. New Applications of Weak Donor Atoms to Coordination, Organometallic and Materials Chemistry. *Comments Inorg. Chem.* **1992**, *13*, 313–357. [CrossRef]
35. Cosier, J.; Glazer, A.M. A nitrogen-gas-stream cryostat for general X-ray diffraction studies. *J. Appl. Crystallogr.* **1986**, *19*, 105–107. [CrossRef]
36. Sheldrick, G.M. A short history of SHELX. *Acta Crystallogr. Sect. A: Found. Crystallogr.* **2008**, *64*, 112–122. [CrossRef]
37. Dolomanov, O.V.; Bourhis, L.J.; Gildea, R.J.; Howard, J.A.K.; Puschmann, H. OLEX2: A complete structure solution, refinement and analysis program. *J. Appl. Crystallogr.* **2009**, *42*, 339–341. [CrossRef]
38. Dolomanov, O.V.; Blake, A.J.; Champness, N.R.; Schroder, M. OLEX: New software for visualization and analysis of extended crystal structures. *J. Appl. Crystallogr.* **2003**, *36*, 1283–1284. [CrossRef]
39. Sheldrick, G.M. Crystal structure refinement with SHELXL. *Acta Cryst.* **2015**, *C71*, 3–8.
40. Sheldrick, G.M. SHELXT—Integrated space-group and crystal-structure determination. *Acta Cryst.* **2015**, *A71*, 3–8. [CrossRef]
41. Available online: http://checkcif.iucr.org (accessed on 15 September 2023).
42. Fonseca Guerra, C.; Snijders, J.G.; te Velde, G.; Baerends, E.J. Towards an order-N DFT method. *Theor. Chem. Acc.* **1998**, *99*, 391–403. [CrossRef]
43. te Velde, G.; Bickelhaupt, F.M.; van Gisbergen, S.J.A.; Fonseca Guerra, C.; Baerends, E.J.; Snijders, J.G.; Ziegler, T. Chemistry with ADF. *J. Comput. Chem.* **2001**, *22*, 931–967. [CrossRef]
44. Vosko, S.H.; Wilk, L.; Nusair, M. Accurate spin-dependent electron liquid correlation energies for local spin density calculations: A critical analysis. *Can. J. Phys.* **1980**, *58*, 1200–1211. [CrossRef]

45. Becke, A.D. Density-functional exchange-energy approximation with correct asymptotic behavior. *Phys. Rev. A* **1988**, *38*, 3098–3100. [CrossRef]
46. Perdew, J.P. Density-functional approximation for the correlation energy of the inhomogeneous electron gas. *Phys. Rev. B* **1986**, *33*, 8822–8824. [CrossRef]